



## **STRUCTURAL PATTERN CONTROLLING THE LOCALIZATION OF RADIOACTIVE MINERALIZATIONS AT GABAL GATTAR AND WADI RAS ABDA AREAS, NORTHERN EASTERN DESERT, EGYPT**

Anton G. Waheeb<sup>1</sup>

**Abstract-** The northern domain of the Egyptian Eastern Desert is characterized by felsic-dominated magmatism formed in the last stage of the shield evolution when a fundamental transition in tectonic style from compressional to extensional occurred and was considered as a high potential source for radioactive minerals such as Meta-aluminous leucogranite highly fractionated A-type granite in Gattar area and alkali feldspar high-K calc-alkaline perthitic granite of W. Ras Abda area. Uranium mineralizations associated with the above-mentioned granitic rocks are mainly intragranitic subtype of hydrothermal vein-type and controlled by tectonic faults. The direction of the maximum resolved shear stress on the intragranitic mineralized tectonic faults at G. Gattar and W. Ras Abda areas indicates that the direction of maximum resolved shear stress ( $\tau$ ) (the direction of stress required to initiate slip) on both G. Gattar and W. Ras Abda intragranitic uranium mineralized fault zones is the same, revealing a monophasic deformation for both areas and is directed NNE-SSW to NE-SW.

**Keywords:** - Direction of shear, uranium, thorium, structurally controlled mineralized faults, G.Gattar and W.Ras Abda areas.

### I. INTRODUCTION

The investigated areas are located in the northern Eastern Desert. The nearest town is Hurghada for the G.Gattar area; while Safage for W.Ras Abda area. The latitude and longitude of G. Gattar area is the intersection of Latitude 27° 7' 30" N and Longitude 33° 17' 5" E while W.Ras Abda granite is bounded by latitudes 26° 43' 22" to 26° 43' 30" N and longitudes 33° 45' 35" to 33° 45' 52"E (Fig.1).

The behavior of uranium and thorium during the formation of igneous rocks indicates a higher concentration in the youngest and most felsic and silicic members. Among felsic igneous rocks, three types may constitute uranium sources for the genesis of uranium deposits with uranium contents well above the Clarke value (3–4 ppm): 1) highly fractionated peralkaline rocks, 2) metaluminous high-K alkaline to calc-alkaline rocks and 3) peraluminous igneous rocks derived from a low degree of melting of supracrustals (Cuney, 2009). They were regarded as the source of uranium all over World (France: Scaillet et al., 1996; Namibia: Nex et al., 2001; Germany: Dill et al., 2010; China; Zhao et al., 2011; Ukraine: Cuney et al., 2012).

The northern domain of the Egyptian Eastern Desert is characterized by felsic-dominated magmatism that represents the magmatic activity marking the end of the cratonization process of the Pan African orogeny, which formed in the last stage of the shield evolution, when a fundamental transition in tectonic style, from compressional to extensional, occurred 620–600 My ago (Stern, 1994; Meert, 2003) and is considered a high potential source for radioactive minerals such as Meta-aluminous leucogranite highly fractionated A-type granite at Gattar area (El Kammar et al., 2001), alkali feldspar high-K calc-alkaline perthitic granite of W. Ras Abda area (Abdel Hamid et al., 2018). They originated from calc-alkaline to alkaline magma in the post-orogenic environment area.

<sup>1</sup>Department of Subsurface Geology, Nuclear Materials Authority, Cairo, Egypt.

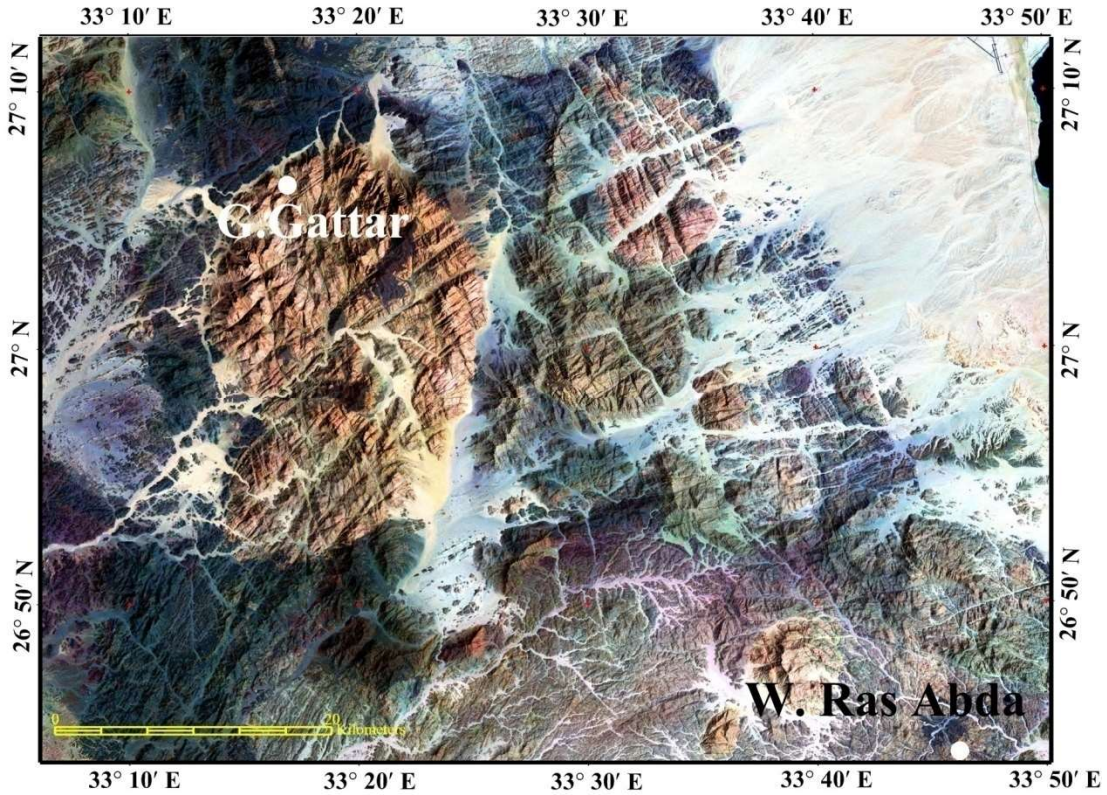


Fig. 1: Land sat image of G. Gattar and W. Ras Abda granitic intrusions

Uranium mineralization associated with the granitic rocks in Egypt is mainly of the hydrothermal vein type, mainly controlled by tectonic faults (Cuney, 2003). Vein uranium deposits are classified (IAEA 2013 classification) as intragranitic or perigranitic subtypes of granite-related uranium deposits (Fig.2).

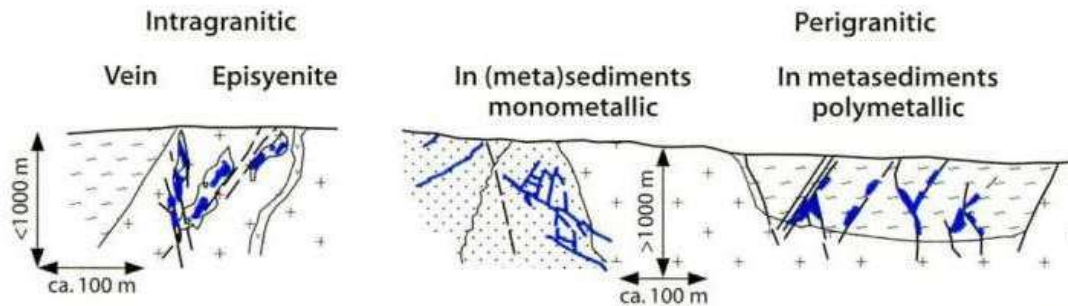


Fig 2: Granite-related uranium deposit type classified into intragranitic and perigranitic sub-types [Dahlkamp2009].

The above-mentioned granite-related uranium occurrences are intragranitic sub-types of granite-related uranium deposit type in the Northern Eastern Desert of Egypt. The uranium content of the G. Gattar granite area is with an average of 11.3ppm (El sundoly and Waheeb 2015) suggesting a fertile-U source. They are regarded as the source of uranium. In addition to that, W .RasAbda granite is characterized by its high content of thorium more than uranium, where the average of eU is 14.3 ppm while that of eTh is 37.6 ppm(Omran, 2005, Omran, 2015 and El Hadary et al ., 2013) suggesting a fertile-Th source.

In this contribution, directions of the shear were carried out to elucidate the main stress required to initiate slip on the intragranitic uranium mineralized fault planes of the investigated areas.

## II. GEOLOGY

W. Ras Abda area is characterized by the presence of two main rock types: older granite intruded by microgranite. These rock types are intruded by different types of dykes associated with pegmatite and quartz veins (Fig. 3). The older granites are widely distributed with moderately to low-relief, highly sheared, and jointed masses of tonalite to granodiorite. They are coarse-grained gray to grayish-white in color.

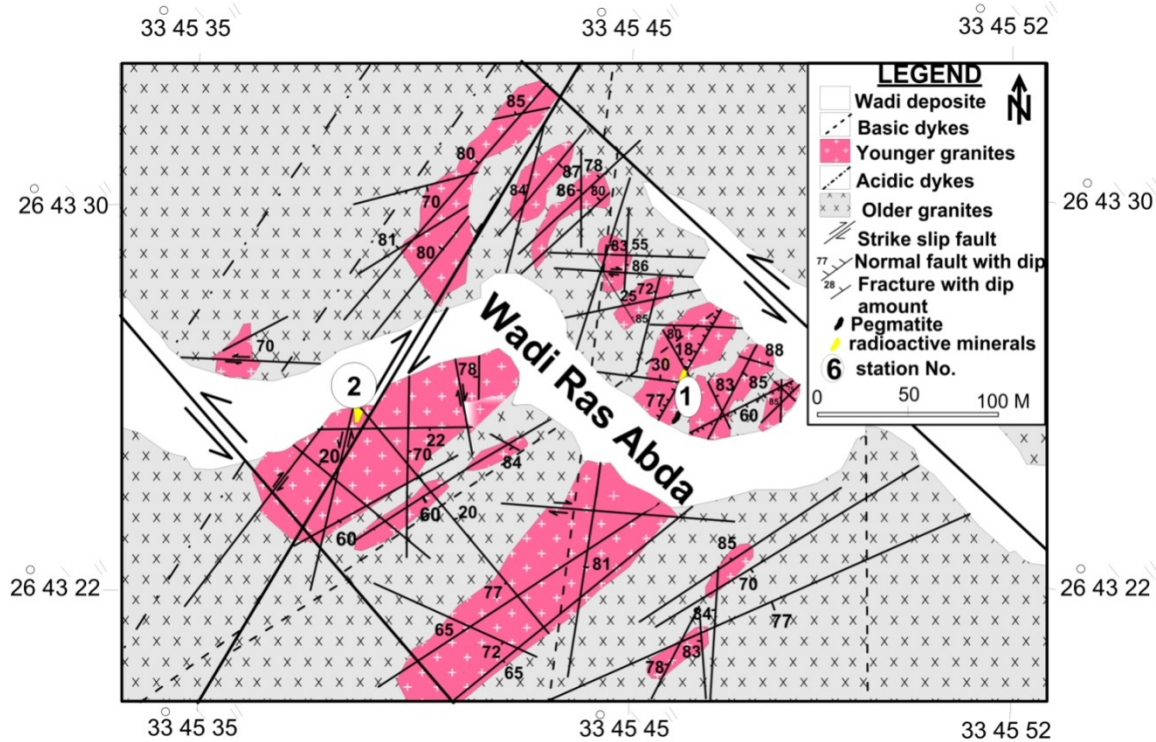


Fig.3 :Geological and structural maps for W.Ras Abda granitic intrusions [after Waheeb and El Sundoly 2020].

W. Ras Abda area microgranite is fine-grained alkali feldspar granite intruding the older granite with sharp intrusive contact ( Fig.4). It occurs as elongated elliptical-shaped bodies striking NE-SW (Fig.3).

G. Gattar area is characterized by the presence of alkali feldspar granite intruded by only basic dykes with quartz veins(Fig.5). They are coarse to medium-grained granites, light pink to reddish-pink in color. They are highly fractured and jointed granites with moderately high rugged mountains (Fig.6).

G.Gattar granite and W. Ras Abda microgranite show highly altered features along fault zones and joint planes such as hematization, kaolinitization, and manganese dendrites due to the effect of hydrothermal solutions. In some mineralized zones, there is some deposition of yellow-color secondary uranium minerals staining the joints and fault planes of the altered rocks in the two areas, while in W. Ras Abda area, the rare metal minerals show brownish-black and reddish-brown colors due to the intensity of hematization and they occur either as mineral segregations coating fractures or in cavities of microgranite.

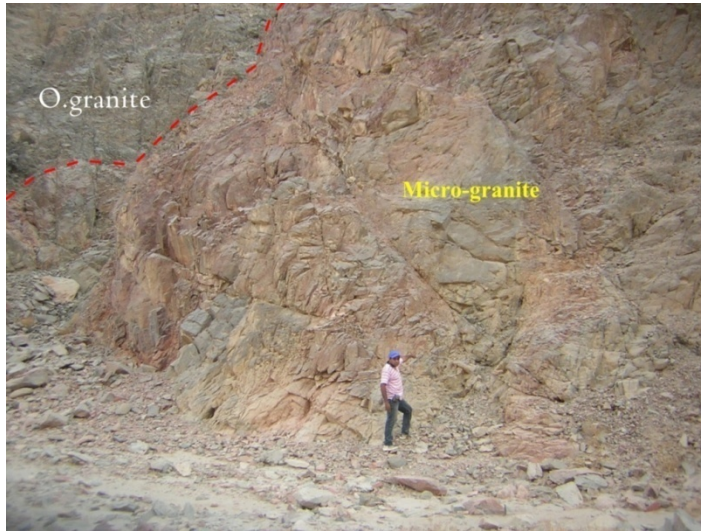


Fig 4: Sharp intrusive contact between older granite (O. granite )and microgranite (Micro-granite), looking SW, W.Ras Abda area.

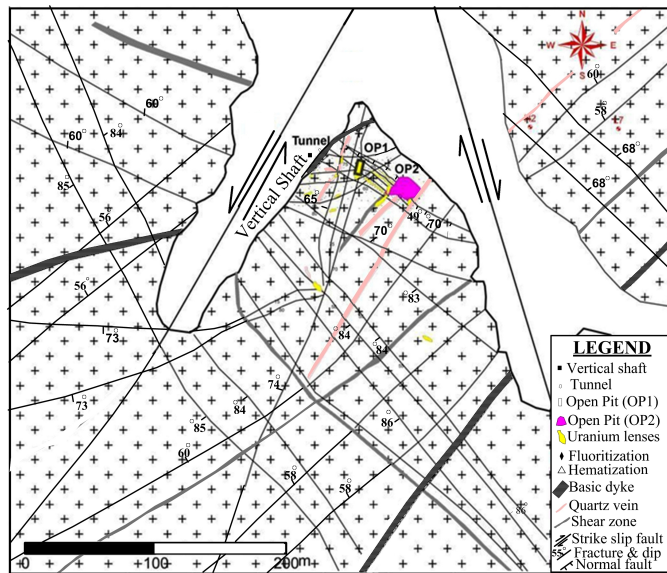


Fig.5: Geological and structural maps for G. Gattar granite [modified after Nossair 2005].

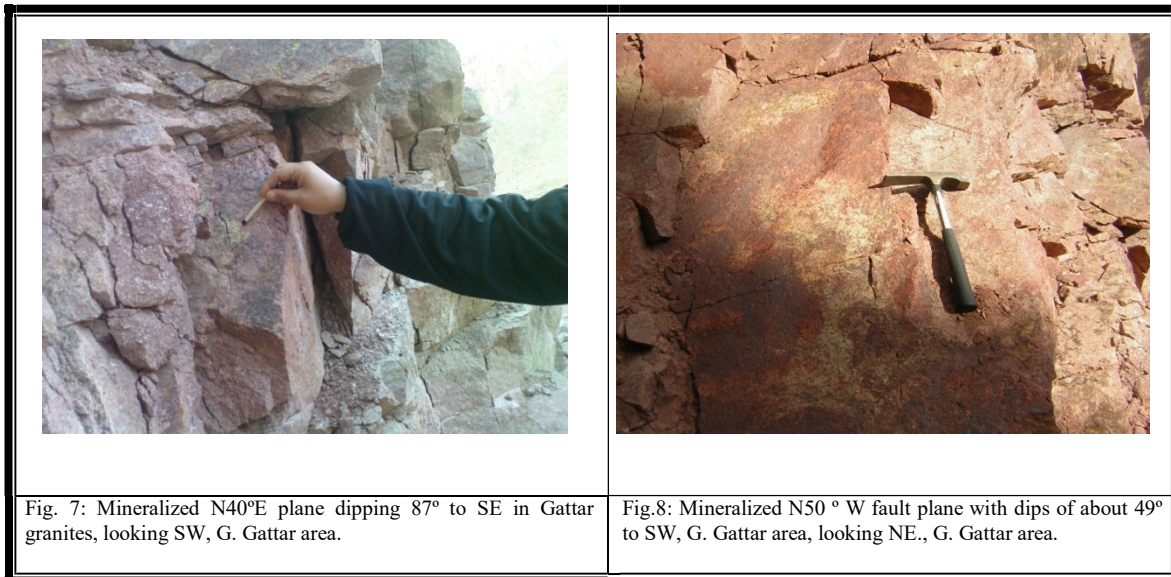


Fig.6: General view of moderately high, rugged mountains of G. Gattar granites, looking SW., G. Gattar area.

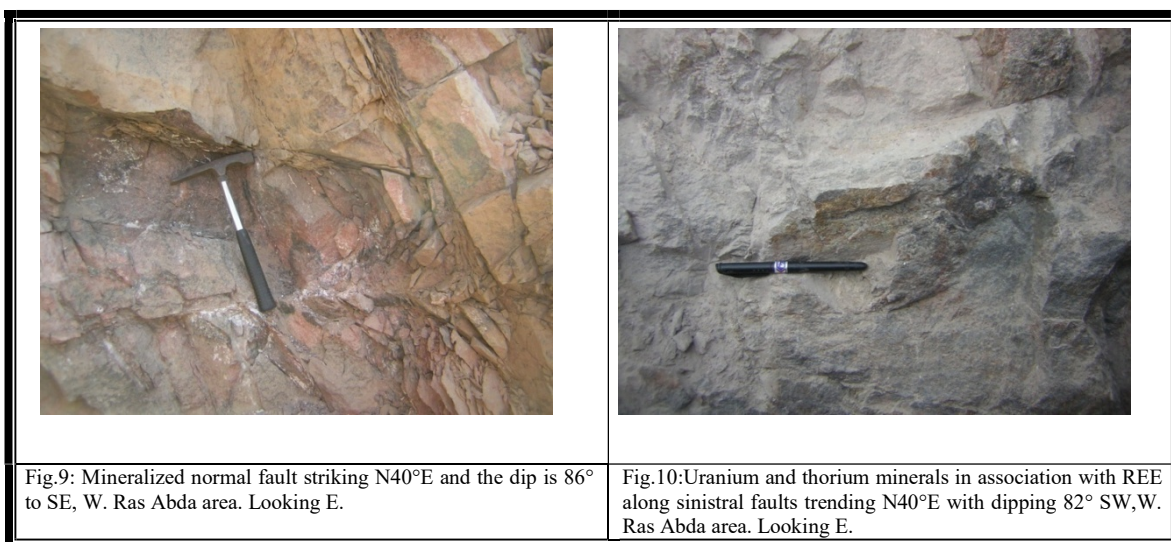
### III.STRUCTURE AND RADIOACTIVITY

At G.Gattar area, the uranium is found along fault zone striking N40°E with a dip of 87° SE(Fig.7). The uranium mineralization is detected containing secondary uranium minerals with eU content equal 450 ppm (El sundoly and Waheeb 2015) and also; along a major fault plane trending N50° W with dips of about 49° to SW (Fig.8). The ESEM study revealed the presence of secondary uranium mineral:uranophane and beta-uranophane with eU content of 400 ppm(El sundoly and Waheeb 2015).

In W. Ras Abda area, the radioactive mineralization is detected along a normal fault striking N40°E and the dip is 86° to SE (Fig.9). Thorite (ThSiO<sub>4</sub>) is the abundant radioactive mineral in this occurrence as identified by (ESEM). EDAX analysis of thorite confirmed the presence of Th = 61.17% and Si =17.68% and was associated with a minor content of U = 8.65 % (Waheeb and El Sundoly 2020). Furthermore, it was recorded along a strike-slip fault trending N40°E with a dip of 82°SW. It shows high radioactive measurements with visible secondary uranium and thorium minerals in addition to the deposition of black rare earth metal (REE) minerals (Fig.10).



Shan, Y, et al (2009) graphical method is used to determine the direction of the main stress required to initiate slip on the above-mentioned intragranitic uranium occurrences.



#### IV. METHODOLOGIES

The direction of the maximum resolved shear stress on a fault plane can be determined by using Shan, Y, et al (2009) graphical method. It differs from preexisting graphical methods in using the direction perpendicular to the maximum resolved shear. It is based upon the theory of vector manipulation, making the proposed method more straightforward and more graphical, and, hence, we believe it more accessible. It is performed in the following steps:-

(1) Plot on a stereogram the principal axes and the normal ( $n$ ) to the fault plane and draw the great circles of the fault plane and the principal stress plane containing  $\sigma_1$  and  $\sigma_2$ .

(2) Draw a great circle through  $n$  to  $\sigma_3$  and mark point  $p$  at its intersection with the  $\sigma_1$   $\sigma_2$  plane. Read along the great circle the angle ( $\theta$ ) between  $p$  and  $\sigma_1$  and mark point  $q$  perpendicular in the  $\sigma_1$   $\sigma_2$  plane to  $p$ . The projection of  $I$  on the principal plane is  $q$  for  $\Phi=1$  and  $\sigma_2$  for  $\Phi=0$ .

(3) Draw an X-Y graph to show points  $p$  and  $q$  projected onto the  $\sigma_1$   $\sigma_2$  plane. The vectors of  $p$  and  $q$  might have X-Y coordinates  $[n_1, n_2]$  and  $[n_2, n_1]$ , respectively. They have non-unit lengths and are mutually perpendicular. Keep in mind that we are interested in the absolute value of angles. Rescale the X-coordinate of  $q$  to  $\Phi n_2$ , to give point  $r$ ,  $[\Phi n_2, n_1]$ . Read the acute angle ( $\phi$ ) between  $r$  and  $\sigma_1$ .

(4) Mark the direction of  $r$  on the stereogram at an angle  $\phi$  from  $\sigma_1$  on the  $\sigma_1$   $\sigma_2$  plane.

(5) Draw a great circle through  $r$  and  $\sigma_3$  and mark its intersection point  $I$  with the great circle of the fault plane. Find the direction of the maximum resolved shear stress ( $\tau$ ), which is perpendicular to  $I$  on the great circle of the fault plane.

(6) Identify each of the sides of the fault plane that has the end of  $\tau$  within  $90^\circ$  of  $\sigma_1$  and  $\sigma_3$  and determine the shear sense by the criterion that the stress acts from the end of  $\tau$  within  $90^\circ$  of  $\sigma_1$  to the end of  $\tau$  within  $90^\circ$  of  $\sigma_3$  (Fry, 1992).

The orientations of the principal stress axes and the ratio of the principle stress differences are obtained by the faults slip straine paleostress analysis by using the computer program Win Tensor, Delvaux and Sperner(2003).

#### V. RESULTS

##### 5.1. MAXIMUM RESOLVED SHEAR STRESS ( $\tau$ ):-

The direction of the maximum resolved shear stress on the fault plane can be obtained from its perpendicular direction on the plane determined graphically by using the Shan, Y, et al (2009) method as mentioned above. This method is different from all existing methods that try a variety of ways to locate the shear direction directly. It is based upon the theory of vector manipulation, and, more importantly, requires far less specialized knowledge about the stress tensor, as mentioned below, than is necessary for many existing graphical methods (e.g., Means, 1989; Fry, 1992; Lisle, 1989, 1998). Accordingly, the calculation is reduced to a greater degree than any of the existing graphical methods, needing no reference to a calculator for the solution of the trigonometrical functions. So, this method is more straightforward and even more graphical.

The direction of the maximum resolved shear stress on the fault plane is done for the intragranitic mineralized fault zones along which the uranium minerals are emplaced in both G. Gattar granite and W.Ras Abda granites.

At the G. Gattar area, the principal stresses,  $\sigma_1$ ,  $\sigma_2$  and  $\sigma_3$  plunge  $9^\circ$  on bearing  $39^\circ$ ,  $81^\circ$  on bearing  $219^\circ$  and  $1^\circ$  on bearing  $130^\circ$  respectively. The stress ratio is 0.5 for the NE-SW intragranitic mineralized fault; while for the NW-SE mineralized fault, the three principal stresses  $\sigma_1$ ,  $\sigma_2$  and  $\sigma_3$  plunge  $72^\circ$  on bearing  $292^\circ$ ,  $16^\circ$  on bearing  $129^\circ$  and  $4^\circ$  on bearing  $38^\circ$  respectively. The stress ratio is 0.5. Finally, W. Ras Abda area, the principal stresses,  $\sigma_1$ ,  $\sigma_2$  and  $\sigma_3$  plunge  $51^\circ$  on bearing  $283^\circ$ ,  $13^\circ$  on bearing  $29^\circ$  and  $36^\circ$  on bearing  $129^\circ$  respectively. The stress ratio is 0 for the mineralized  $N40^\circ E$  normal fault with dipping  $86^\circ$  to SE but the principal stresses,  $\sigma_1$ ,  $\sigma_2$  and  $\sigma_3$  plunges  $17^\circ$  on bearing  $355^\circ$ ,  $73^\circ$  on bearing  $191^\circ$  and  $4^\circ$  on bearing  $86^\circ$  respectively. The stress ratio is 0.5 for the mineralized  $N40^\circ E$  sinistral strike slip fault with dipping  $82^\circ$  to SE.

At G. Gattar area, the direction of maximum resolved shear stress ( $\tau$ ) plunges  $32^\circ$  on bearing  $218^\circ$  (NE-SW) for the  $N40^\circ E$  with dips of about  $87^\circ$  to SE (Fig. 11) and the direction of maximum resolved shear stress ( $\tau$ ) plunges  $47^\circ$  on bearing  $200^\circ$  (NNE-SSW) for the  $N50^\circ W$  with dips of about  $49^\circ$  to SW (Fig. 12).

At W. Ras Abda area, the direction of maximum resolved shear stress ( $\tau$ ) plunges  $60^\circ$  on bearing  $213^\circ$  (NNE-SSW) for  $N40^\circ E$  normal fault with dipping  $86^\circ$  to SE (Fig.13), and the direction of maximum resolved shear stress ( $\tau$ ) plunges  $21^\circ$  on bearing  $42^\circ$  (NE-SW) for the mineralized  $N40^\circ E$  sinistral strike slip fault with dipping  $82^\circ$  to SE (Fig. 14).

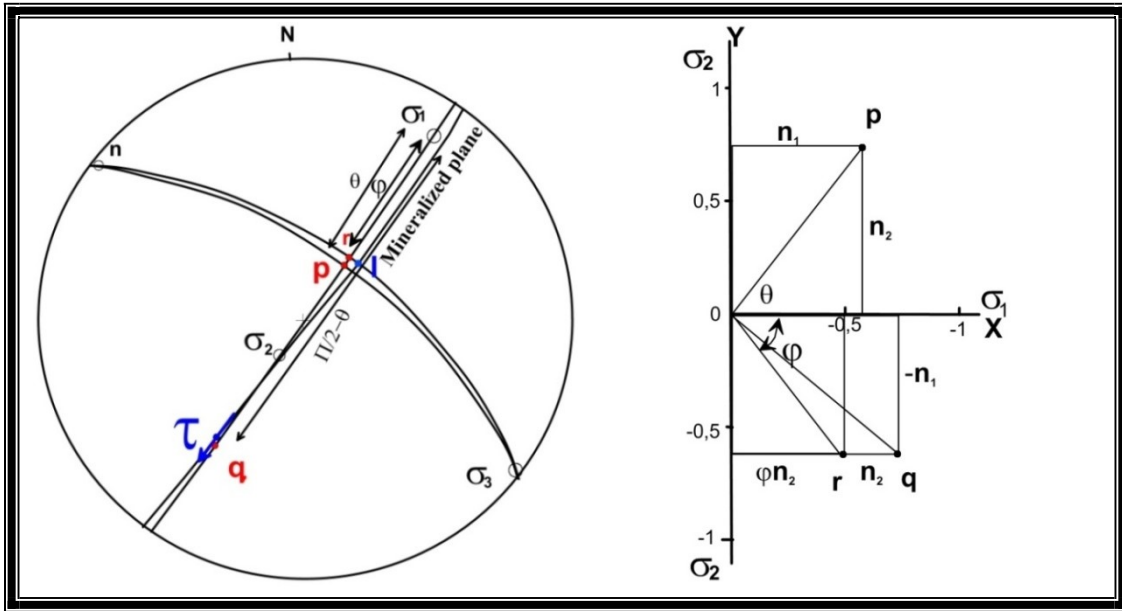


Fig. 11: Graphical method to determine the direction of shear( $\tau$ ) on the intragranitic mineralized NE-SW fault plane at G. Gattar area.

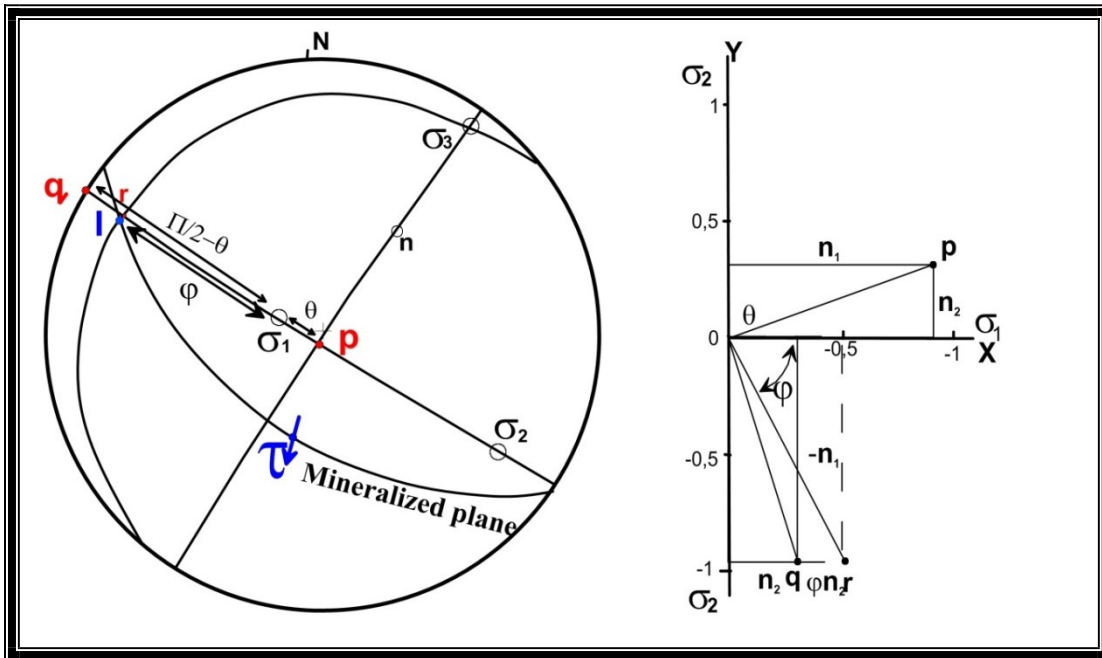


Fig. 12: Graphical method to determine the direction of shear( $\tau$ ) on the intragranitic mineralized NW-SE fault plane at G. Gattar area.

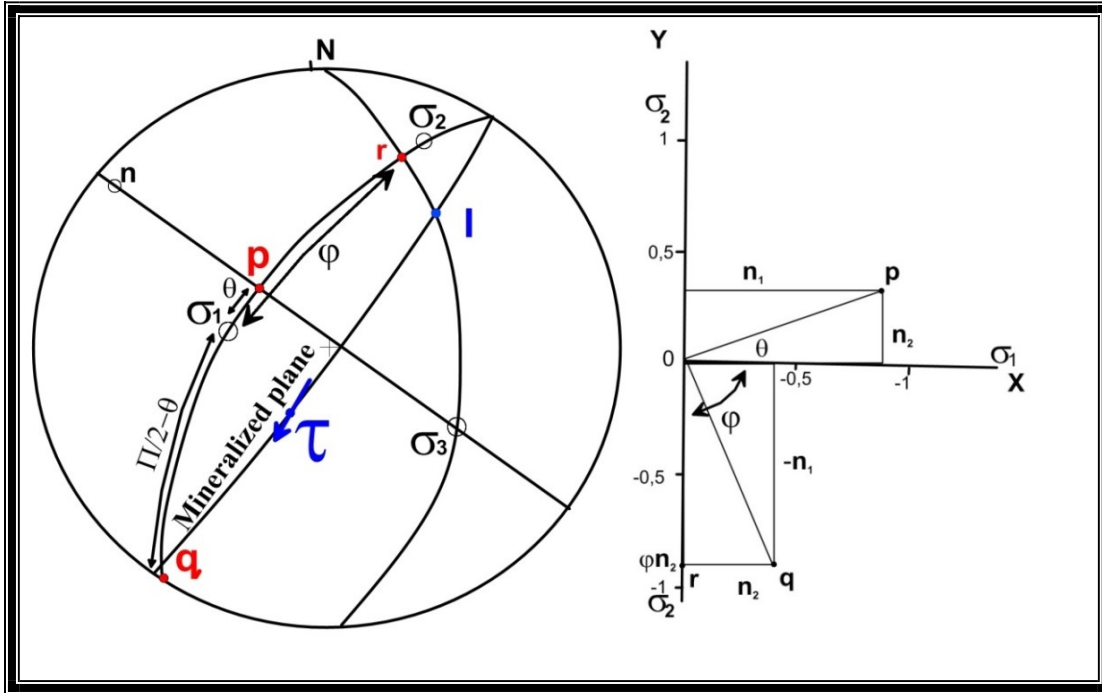


Fig.13:Graphical method to determine the direction of shear ( $\tau$ ) on intragranitic mineralized N40°E normal fault with dipping 86° to SE at W. Ras Abda area.

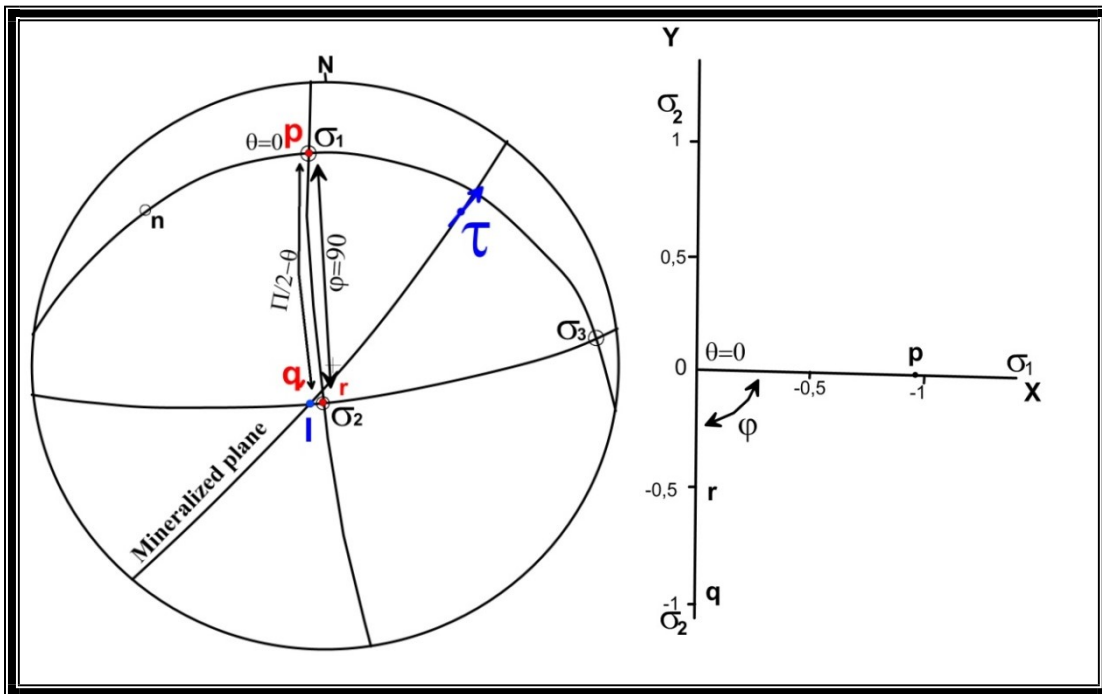


Fig. 14:Graphical method to determine the direction of shear ( $\tau$ ) on the intragranitic mineralized N40°E sinistral strike slip fault with dipping 82° to SE at W. Ras Abda area.

The above-mentioned structural analysis indicates that the direction of maximum resolved shear stress ( $\tau$ ) on both G. Gattar and W. Ras Abdaintragranitic uranium mineralized fault zones is directed NNE-SSW to NE-SW.



## VI. DISCUSSION

At G. Gattar area the uranium is found along strike slip fault zone striking N40°E with dipping equal 87° SE and along a major normal fault plane trending N50° W with dips of about 49° to SW. At W. Ras Abda area, the radioactive mineralization is detected along a normal fault striking N40°E and the dip is 86° to SE. As well as, strike slip fault trending N40°E with dipping 82°SW.

It is clear that the main structure fabric elements which control the distribution and localization of radioactive mineralization are mainly of two trends the first trend is NE-SW and the other trend is NW-SE with very steep dip angles. The NE-SW structural control trend has nearly the same attitude at G. Gattar and W. Ras Abda area.

The direction of the maximum resolved shear stress ( $\tau$ ) for the intragranitic mineralized fault zones along which the uranium minerals are emplaced in the investigated areas indicates that there is a similarity between G. Gattar and W. Ras Abda area in the direction of the maximum resolved shear stress and it is directed NNE-SSW to NE-SW. At G. Gattar area, the direction of maximum resolved shear stress ( $\tau$ ) plunges 47° on bearing 200° (NNE-SSW) and plunges 32° on bearing 218° (NE-SW) and at W. Ras Abda area, the direction of maximum resolved shear stress ( $\tau$ ) plunges 60° on bearing 213° (NNE-SSW) and plunges 21° on bearing 42° (NE-SW). This shear stress ( $\tau$ ) could be syncontemporaries with the youngest extensional force of Red Sea rift which affected Egypt (Khalil and McClay, 1998).

## VII. CONCLUSION

The presence of potential uranium and thorium mineralizations in different occurrences of the above-mentioned younger granites are greatly affected by the presence of strong internal tectonics which offered good preparation of the sites for mineralization. The various uranium and thorium occurrences are mostly controlled by fault zones. They are occasionally associated with a wide range of wall-rock alteration features.

The direction of the maximum resolved shear stress on the fault planes is done for the intragranitic mineralized fault zones; which are considered the most important zones along which the uranium minerals are emplaced in both G. Gattar granite and W. Ras Abda granites.

This structural analysis indicates that the direction of maximum resolved shear stress ( $\tau$ ) on both G. Gattar and W. Ras Abda intragranitic uranium mineralized fault zones are the same (monophase of deformation) and it is directed NNE-SSW to NE-SW could be related to the Red Sea rifting. So, it could be concluded that the Red Sea rift plays a great role in the distribution and localization of uranium minerals in G. Gattar and W. Ras Abda areas.

## REFERENCES

- [1] Abdel Hamid, A. A., El Sundoly, H. I. and Abu Steet, A. A. 2018: Hydrothermal alteration and evolution of Zr-Th-U-REE mineralization in the microgranite of Wadi Ras Abda, North Eastern Desert, Egypt. *Arabian Journal of Geosciences*. <https://doi.org/10.1007/s12517-018-3623-2>.
- [2] Bentor, Y.K., 1985: The crustal evolution of the Arabo-Nubian Massif with special reference to the Sinai Peninsula. *Precambrian Research* 28: 1–74.
- [3] Cuney, M., 2003: Uranium potential of Eastern Desert granite, Egypt. Unpublished Internal Report, Nuclear Materials Authority, Cairo, Egypt.
- [4] Cuney, M., 2009: The extreme diversity of uranium deposits. *Mineralium Deposita*, 44, 3–9.
- [5] Cuney, M., Emetz, A., Mercadier, J., Mykchaylov, V., Shunko, V. and Anatoliy Yushenko, A., 2012: Uranium deposits associated with Nametasomatism from central Ukraine: A review of some of the major deposits and genetic constraints. *Ore Geol. Rev.* 44: 82–106.
- [6] Dahlkamp, F.J., 2009: *Uranium Deposits of World: Asia*. Springer, p. 493.
- [7] Delvaux, D. and Sperner, B., 2003: New aspects of tectonic stress inversion with reference to the TENSOR program. *Geological Society, London, Special Publications*, v. 212, pp. 75–100.
- [8] Dill, H. G., A. Gerdes, A. Weber, B., 2010: Age and mineralogy of supergene uranium minerals—Tools to unravel geomorphological and palaeohydrological processes in granitic terrains (Bohemian Massif, SE Germany). *Geomorphology* 117: 44–65.
- [9] EL Hadary A., El Azab A. and Omran A.A., 2013: Contributions to the geology and mineralogy of wadi Ras Abda area, North Eastern Desert, Egypt. *Nuclear Sciences Scientific Journal*. V. 2.
- [10] El-Kammar, A.M., Salman, A.E., Shalaby, M.H., Mahdy, A.I., 2001: Geochemical and genetical constraints on rare metals mineralizations at the central Eastern Desert of Egypt. *Chemical Journal* 35, pp.117–135.
- [11] El Sundoly, H. I. and Waheeb, A. G., 2015: A New Genetic Model, For The Localization of Uranium Minerals At The Northern part of Gabal Gattar, North Eastern Desert, Egypt. 3<sup>rd</sup> Symposium of the Geol. Res. in the Tethys Realm, Cairo Univ. 21–39.
- [12] Fry, N., 1992: Direction of shear. *J. Struct. Geol.*, Vol 14, pp.253–255.
- [13] Genna, A., Nehlig, P., Le Goff, E., Guerrot, C. and Shanti, M., 2002: Proterozoic tectonism of the Arabian Shield. *Precambrian Research* 117: 21–40.
- [14] IAEA 2013: Uranium deposit classification. Vienna, Austria
- [15] Khalil, S. M. and McClay, K., (1998): Structural architecture of the eastern margin of the gulf of Suez: field studies and analogue modeling results. In proceedings of 14th Exploration Conference, October, 1998. Vol.1. Egyptian General Petroleum Corporation, Cairo: 201–211.

- [16] Kröner, A., Greiling, R., Reischmann, T., Hussein, I.M., Stern, R.J., Durr, S., Krugger, J. and Zimmer, M., 1987: Pan-African crustal evolution in the Nubian segment of north-eastern Africa. In: Kröner, A. (Ed.), Proterozoic Lithospheric Evolution Am. Geophys. Union Geodynamic Series 15, p. 235–257.
- [17] Lisle, R.J., 1989: A simple construction for shear stress. *J. Struc. Geol.*, Vol. 11, pp.493–495.
- [18] Lisle, R.J. 1998:simple graphical constructions for the direction of shear *J. Struc. Geol.*, Vol.20, No.7, pp. 969 - 973.
- [19] Means, W.D., 1989:A construction for shear stress on a generally-oriented plane. *Journal of Structural Geology* 11, 625–627
- [20] Meert, J.G., 2003: A synopsis of events related to the assembly of eastern Gondwana. *Tectonophysics* 362: 1–40.
- [21] Nex, P. A., Kinnaird, J. A., Oliver, G. J., 2001: Petrology, geochemistry and uranium mineralization of post-collisional magmatism around Goanikontes, southern Central Zone, Damaran Orogen, Namibia. *Journal of African Earth Sciences* 33: 481–502.
- [22] Nossair,A.A. 2005: Geological factors controlling uranium distribution and affecting its localization in G-II occurrence , GabalQattar , North Eastern Desert, Egypt.M.Sc. thesis, Zagazig Univ.,Banha Branch,Zagazig, Egypt. 181 p
- [23] Omran A. A. 2005:Geological, petrochemical studies and potentiality of uranium-thorium occurrences in Gabal Um Taghir El-Tahtani area with an emphasis on the granitic rocks, Central Eastern Desert, Egypt. Ph.D. thesis, Ain Shams Univ., Cairo, Egypt. 189 p
- [24] Omran,A, A., 2015:Geology, mineralogy and radioelements potentiality of microgranite dykes to the south of Wadi Abu Haded area, Northern Eastern Desert, Egypt. *Al-Azhar Bull Sci* 26:67–89
- [25] Scaillet, S., Cuney, M., Le Carlier De Veslud, C., Cheilletz, A. andRoyer, J. J., 1996: Cooling pattern and mineralization history of Saint Sylvester and western Marche leucogranite pluton, French Massif Central: II. Thermal modeling and implications for the mechanisms of uranium mineralization. *Geochimica et Cosmochimica, Acta* 60: 4673-4688.
- [26] Stern, R.J., 1994: Arc-assembly and continental collision in the Neoproterozoic African orogeny: implications for the consolidation of Gondwanaland. *Annual Review of Earth and Planetary Sciences*, 22, 319–351.
- [27] Stern, R. J., Gottfried, D. and Hedge, C. E., 1984: Late Precambrian rifting and crustal evolution in the Northeastern Desert of Egypt. *Geology* 12: 168-172.
- [28] Shan, Y., Fry, N., Lisle. R.L., 2009:Graphical construction for the direction of shear. *J. Struc. Geol.*, Vol.31, pp. 476- 478.
- [29] Waheeb, A. G. and El Sundoly, H. I., 2020: Tensile stress and related Th-U-REE mineralizations in the granite of Wadi Ras Abda, North Eastern Desert, Egypt.. *Arabian Journal of Geosciences*. <https://doi.org/10.1007/s12517-020-05543-z>.
- [30] Zhao, K., Jiang, S., Dong, C., Chen, W., Chen, P., Ling, H., Zhang, J., Kai-Xing Wang, K., 2011: Uranium-bearing and barren granites from the Taoshan Complex, Jiangxi Province, South China: Geochemical and petrogenetic discrimination and exploration significance. *Journal of Geochemical Exploration* 110: 126–135.